Inorganic Chemistry

ARTICLE

pubs.acs.org/IC

Synthesis, Molecular and Electronic Structures of Six-Coordinate Transition Metal (Mn, Fe, Co, Ni, Cu, and Zn) Complexes with Redox-Active 9-Hydroxyphenoxazin-1-one Ligands

Eugeny P. Ivakhnenko,[†] Andrey G. Starikov,[‡] Vladimir I. Minkin,[*,†] Konstantin A. Lyssenko,[§] Mikhail Yu. Antipin,[§] Vladimir I. Simakov,[†] Mikhail S. Korobov,[†] Gennady S. Borodkin,[†] and Pavel A. Knyazev[†]

[†]Institute of Physical and Organic Chemistry, Southern Federal University, 194/2 Stachka Ave. 344090 Rostov on Don, Russian Federation

[‡]Southern Scientific Center of Russian Academy of Sciences, 194/2 Stachka Ave. 344090 Rostov on Don, Russian Federation

[§]A.N. Nesmeyanov Institute of Organoelement Compounds of Russian Academy of Sciences, 28 Vavilov St. 119991, Moscow, Russian Federation

Supporting Information

ABSTRACT: A series of pseudo-octahedral metal (M = Mn, Fe, Co, Ni, Cu, Zn) complexes **4** of a new redox-active ligand, 2,4,6,8-tetra(*tert*-butyl)-9-hydroxyphenoxazin-1-one **3**, have been synthesized, and their molecular structures determined with help of X-ray crystallography. The effective magnetic moments of complexes **4** (M = Mn, Fe, Co, and Ni) measured in the solid state and toluene solution point to the stabilization of their high-spin electronic ground states. Detailed information on the electronic structure of the complexes and their redox-isomeric forms has been obtained using density functional theory (DFT) B3LYP*/6-311++G(d,p) calculations. The energy disfavored low-spin structures of manganese, iron, and cobalt complexes have been located, and based on the computed geometries and distribution of spin densities identified as $Mn^{IV}[(Cat\text{-}N\text{-}SQ)]_2$, $Fe^{II}[Cat\text{-}N\text{-}BQ)]_2$, and $Co^{II}[Cat\text{-}N\text{-}BQ)]_2$ compounds, respectively. It has been shown that stabilization of the high-spin structures of complexes **4** (M = Mn, Fe, Co) is caused by the rigidity of the molecular framework of ligands **3** that sterically inhibits interconversions between the redox-isomeric forms of the complexes. The calculations performed on complex **4** (M = Co) predict that a suitable structural modification that might provide for stabilization of the low-spin electromeric forms and create conditions for the valence tautomeric rearrangement via stabilization of the low-spin electromer and narrowing energy gap between the low-spin ground state tautomer and the minimal energy crossing point on the intersection of the potential energy surfaces of the interconverting structures consists in the replacement of an oxygen in the oxazine ring by a bulkier sulfur atom.

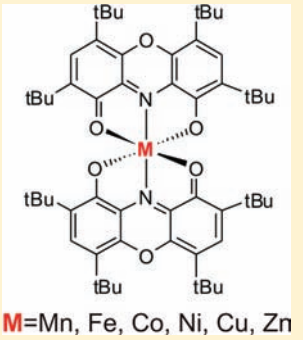

INTRODUCTION

Metal complexes exhibiting intramolecular electron transfer (IET) between a metal center and a redox-active ligand as induced by external stimuli (valence tautomerism[1]) continue to be under intense investigation because of the interest in their switchable magnetic and optical properties and possible application as constitutive elements of various molecular electronic devices[2] and catalytic systems.[3] The proneness of the electronically labile valence tautomeric complexes based on the redox-active (so-called noninnocent[4]) ligands to thermal and/or photoinitiated rearrangements strongly depends on the interplay between the frontier orbitals located at the metal center and the ligand. When the energies of these orbitals are comparable, IET is a likely effect in case evolution of the geometry of the ground state electronic isomers (electromers[5]) bringing the system into the region of crossing the potential energy surfaces of the interconverting structures can be achieved at the sufficiently low energy cost (less than ~80 kJ mol^{-1}) in the minimal energy crossing point (MECP).[6] A necessary precondition for a valence tautomeric rearrangement to occur is the low-spin form of the ground state isomer.[1d] The studies of valence tautomerism have been mostly concentrated on six-coordinate transition metal complexes with *o*-quinone-based ligands of the general formula $[M(Q)_2L_2]$, wherein L and L_2 are appropriate mono- and bidentate ligands, typically pyridine and 2,2′-dipyridyl, respectively. The first discovered Co(II)/Co(III) valence tautomeric system belongs to this particular structural type.[7] Another type of the redox-active ligands that may display different oxidation states when coordinated to metallic centers is represented by the tridentate ligands in homoleptic transition metal complexes. In this series, an important place belongs to iminoquinonephenolates **1**, for which four

Received: February 28, 2011
Published: June 30, 2011

dx.doi.org/10.1021/ic2004062 | *Inorg. Chem.* 2011, 50, 7022–7032

oxidation states **1a**−**d** have been found in a variety of transition metal complexes.[1,8]

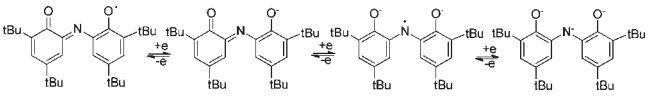

Reversible redox rearrangements in Co and Mn complexes formed by this ligand have been studied for both neutral and cationic systems and shown to occur with relatively low energy barriers of about 42.0 kJ mol^{-1} for Co complex **2** (M = Co).[8] This value has been reasonably well reproduced by the DFT B3LYP*/6-311++G(d,p) calculations[9] allowed to locate the minimal energy crossing point (MECP) at the intersection of the doublet and quartet potential energy surfaces (PESs) at 51.8 kJ mol^{-1} above **2a** (Co(III)-LS, $S = 1/2$). A deeper insight into the intrinsic mechanisms governing the thermally induced IET processes has been recently reached owing to the ab initio complete active space second-order perturbation theory (CASSCF/CASPT2) calculations[10] performed on bis-(iminoquinonephenolate) Co(II), Fe(II), and Ni(II) **2**. It has been shown that Co complex exhibits the coexistence of two IET processes, ligand-to-metal and ligand-to-ligand, whereas only the latter one was found to operate in the Fe complex and no IET was found to take place in the Ni complex. In agreement with the experimental findings the calculations carried out by using the X-ray geometries of Co and Fe complexes point to their low-spin ground state structures **2a** (M = Co) and **2a** (M = Fe), respectively.

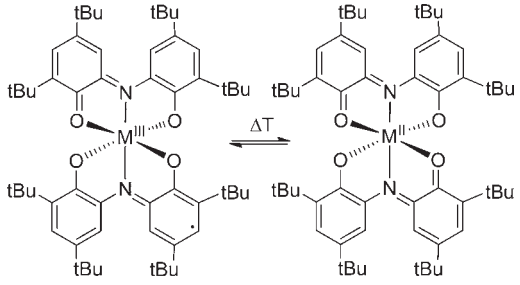

2a **2b**

We have recently developed a method for the preparation of a heterocyclic analogue **3**[11a] of the iminoquinone ligand **1**. A distinguishing feature of the compound **3** is the sterical rigidity of its tricyclic molecular skeleton. With the purpose of gaining insight into the influence of this structural peculiarity on the choice of the ground-state structure, position, and dynamics of the possible valence tautomeric equilibria of 3d-metal complexes formed by the tridentate ligand **3** we have synthesized a systematic series of complexes **4** and studied their molecular and electronic structures with the use of X-ray crystallography, density functional theory calculations, and magnetic and NMR measurements.

EXPERIMENTAL SECTION

Synthesis. 2,4,6,8-Tetra-(*tert*-butyl)-9-hydroxyphenoxazin-1-one 3 was prepared according to the previously reported procedure.[11a] Oxidation of a toluene solution of **3** with potassium ferricyanide accomplished in anaerobic conditions in the resonator of the electron paramagnetic resonance (EPR) spectrometer gives rise to the formation of the phenoxyl radical **3a** which is stable in anaerobic conditions at ambient

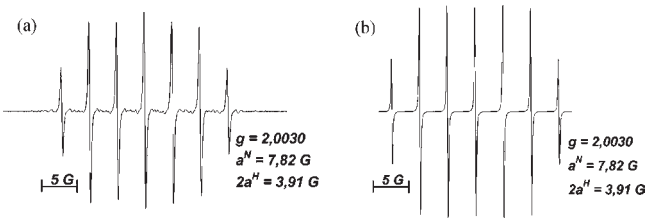

Figure 1. X-band EPR spectrum of **3a**, (BQ-N-SQ) in toluene solution at 293 K (a) and the computer simulation spectrum (b).

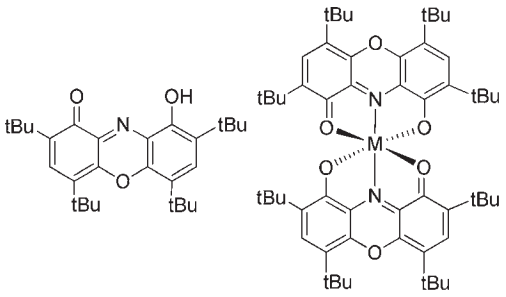

3 **4** M = Mn, Fe, Co, Ni, Cu, Zn

temperature. The X-band EPR spectrum of a toluene solution of **3a** is shown in Figure 1. The same type of EPR spectrum pointing to the formation of **3a** is registered also under irradiation of a toluene solution of **3** with UV-light (mercury lamp LSB610 100 W Hg). The hyperfine split features are due to coupling of the unpaired electron to nuclei of nitrogen ($\alpha^N = 7.82$G) and two hydrogen atoms in the positions of 3 and 7 of the heterocycle ($2\alpha^H = 3.91$G). Reduction of **3** with potassium amalgam in tetrahydrofuran solution results in the formation of radical-dianion **3b** as detected by the EPR spectrum composed of seven lines with $\alpha^N = 6.32$G and $2\alpha^H = 3.43$G. The values of the hyperfine coupling constants observed for **3a** and **3b** are very close to those found for a structurally similar 1-hydroxy-2,4,6,8-tetrakis(*tert*-butyl)phenoxazin-10-yl radical obtained by oxidation of 3,5-di-(*tert*-butyl)-*o*-aminophenol with 3,5-di-(*tert*-butyl)-*o*-benzoquinone.[11b]

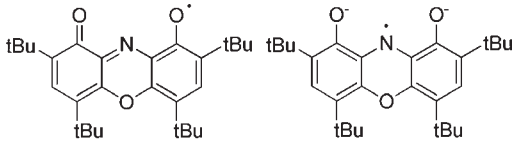

3a, (BQ-N-SQ) **3b**, $(Cat\text{-}N\text{-}SQ)^{-2}\,2K^+$

Bis-[2,4,6,8-tetra-(*tert*-butyl)-9-oxyphenoxazin-1-onolate] metal complexes of general formula 4 denoted as M(bu_4phenoxon)$_2$ (M = Mn, Fe, Co, Ni, Cu, Zn) were prepared by mixing methanol solutions of 22 mg (0.05 mmol) of 2,4,6,8-tetra-(*tert*-butyl)-9-hydroxyphenoxazin-1-one **3** (20 mL) and 0.025 mmol of the appropriate metal(II) acetate M-$(CH_3COO)_2 \cdot nH_2O$ (10 mL). The solution was heated at reflux for 1.5−2 h, cooled to room temperature, and the precipitated crystals of complexes **4** were filtered out, vacuum-dried, and recrystallized from benzene.

*Mn(bu_4phenoxon)$_2$, **4** (M = Mn).* For the preparation of this complex, $Mn(CH_3COO)_2 \cdot 4H_2O$ (6.1 mg, 0.0025 mmol) was used. Blue-green crystals (yield 19.6 mg, 85%). Mp > 360 °C. Anal. Calculated for $C_{56}H_{76}N_2O_6Mn$: C, 72.47; H, 8.25; N, 3.02; Mn, 5.92 Found: C, 72.39; H, 8.19; N, 3.06; Mn, 5.87. ^{1}H NMR (toluene-d_8, 30 °C): $\delta = 2.09$ (b, 72H, *tert*-Bu) ppm. IR(cm^{-1}): 1614(S), 1591(m), 1549(s), 1457(m), 1507(w), 1449(m), 1393(m), 1353(w), 1329(w), 1287(s), 1246(w), 1198(m), 1165(m), 1070(m) 1036(m), 1001(w), 903(s),

dx.doi.org/10.1021/ic2004062 |*Inorg. Chem.* 2011, 50, 7022–7032

Table 1. Crystal and Structure Refinement Data for Complexes 4 (M = Mn, Fe, Co, Ni, Cu, Zn)

	Mn	Fe	Co	Ni	Cu	Zn
formula	$C_{56}H_{76}MnN_2O_6$	$C_{56}H_{76}FeN_2O_6$	$C_{92}H_{112}CoN_2O_6$	$C_{92}H_{112}N_2NiO_6$	$C_{92}H_{112}CuN_2O_6$	$C_{92}H_{112}N_2O_6Zn$
M, $F(000)$	928.13, 1996	929.04, 2000	1400.77, 3012	1400.55, 3016	1405.38, 3020	1407.21, 3024
T, K	100	100	100	100	100	100
crystal system, space group	monoclinic, $C2/c$	monoclinic, $P2_1/c$	orthorhombic, $Pbcn$	orthorhombic, $Pbcn$	orthorhombic, $Pbcn$	orthorhombic, $Pbcn$
$Z(Z')$	4(0.5)	4(1)	4(0.5)	4(0.5)	4(0.5)	4(0.5)
a, Å	23.540(3)	20.545(3)	20.5128(16)	21.056(4)	20.558(10)	20.5359(15)
b, Å	20.047(3)	19.772(3)	18.4721(15)	18.298(3)	18.436(9)	18.5434(14)
c, Å	12.6391(16)	13.059(2)	20.9387(18)	20.642(4)	20.851(8)	21.0061(15)
β, deg	116.672(2)	90.029(3)	90	90	90	90
V, Å^3	5329.6(12)	5304.7(15)	7934.0(11)	7953(3)	7903(6)	7999.2(10)
D_{calc}, g·cm^{-3}, μ, cm^{-1}	1.157, 2.96	1.163, 3.33	1.173, 3.33	1.17, 2.98	1.181, 3.31	1.168, 3.31
$2\theta_{max}$, deg	54	54	58	52	52	56
reflections measured	15761	54156	40393	60560	27923	48019
independent reflections (R_{int})	5810	11588	10542	7817	7757	9652
	(0.0947)	(0.0714)	(0.0715)	(0.0939)	(0.0810)	(0.0956)
observed reflections [$I > 2\sigma(I)$]	2980	5068	6264	4007	4136	4875
R1	0.0435	0.0714	0.0500	0.0622	0.0449	0.0392
wR2	0.0727	0.1669	0.1513	0.1651	0.0617	0.0687
GOF	0.74	0.973	1.055	0.983	0.98	0.791
$\Delta\rho_{max}$, $\Delta\rho_{min}$ (e Å^{-3})	0.303, −0.463	0.324, −0.465	0.727,-0.371	0.872,-0.465	0.521, −0.644	0.438, −0.610

Table 2. Effective Magnetic Moments, μ_{eff}, Measured in the Solid State and in Toluene-d$_8$ Solution at 298 K and Theoretical Values Expected for the High-Spin (μ_{eff} - HS) and Low-Spin (μ_{eff} - LS) Electronic States of Complexes 4

M	μ_{eff}, BM, toluene-d$_8$	μ_{eff}, BM, solid state	μ_{eff} - HS, BM	μ_{eff} - LS, BM
Mn(II)	6.07	5.88	5.92	1.73
Fe(II)	4.88	4.40	4.90	0
Co(II)	4.81[a]	4.52[a]	3.87	1.73
Ni(II)	2.78	3.20	2.83	0
Cu(II)	1.79	1.75	1.73	1.73

[a] The increased values of effective magnetic moments were determined for other high-spin Co(II) complexes with redox-active ligands and were attributed to the enhanced spin−orbit interactions.[19]

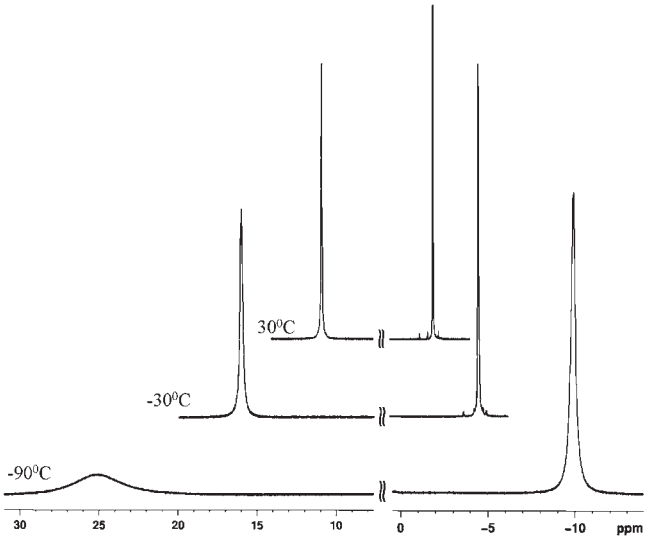

Figure 2. Temperature-dependent *tert*-butyl ^{1}H NMR spectrum (600 MHz) of **4** (M = Co) in toluene-d$_8$. Signals at −9.88, −4.87, and −2.29 ppm belong to the groups in the positions 4 and 6 of the phenoxazine rings. Signals at 25.01, 15.43, and 10.44 ppm belong to the groups in the positions 2 and 8.

877(m), 821(s), 776(s), 741(m), 695(m), 610(s). UV−vis (toluene), λ_{max} (ε, M^{-1} cm^{-1}): 297 (23000), 410 (28000), 786 (20000).

Co(bu$_4$phenoxon)$_2$, ***4*** *(M = Co).* For the preparation of this complex, $Co(CH_3COO)_2 \cdot 4H_2O$ (6.2 mg, 0,0025 mmol) was used. Dark blue crystals (yield 17.6 mg, 76%). Mp > 360 °C. Anal. Calculated for $C_{56}H_{76}N_2O_6Co$: C, 72.16; H, 8.22; N, 3.01; Co, 6.32 Found: C, 72.20; H, 8.25; N, 3.07; Co, 6.30. ^{1}H NMR (toluene-d$_8$, 30 °C): δ = −2.29 (s, 36H, *tert*-Bu), 10.44 (b, 36H, *tert*-Bu) ppm. IR (cm^{-1}): 1589(m), 1540(m), 1499(w), 1481(m), 1384(m), 1355(m), 1325(w), 1284(m), 1245(w), 1197(m), 1163(m), 1093(s), 1069(s), 1037(w), 1005(w), 901(m), 877(m), 776(s), 732(m), 694(m), 608(s). UV−vis (toluene), λ_{max} (ε, M^{-1} cm^{-1}): 293 (24200), 396 (17500), 763 (15800).

Fe(bu$_4$phenoxon)$_2$, ***4*** *(M = Fe).* For the preparation of this complex, $FeCl_2 \cdot 4H_2O$ (5.0 mg, 0.025 mmol) was used. Brown-green crystals (yield 14.6 mg, 63%). Mp > 360 °C. Anal. Calculated for $C_{56}H_{76}N_2O_6Fe$: C, 72.40; H, 8.25; N, 3.02; Fe, 6.01 Found: C, 72.35; H, 8.19; N, 3.08; Fe, 5.96. ^{1}H NMR (toluene-d$_8$, 30 °C): δ = 2.23 (s, 36H, *tert*-Bu), 3.80 (b, 36H, *tert*-Bu) ppm. IR(cm^{-1}): 1582(w), 1541(s), 1525(s), 1495(m), 1478(m), 1400(s), 1361(w), 1313(m), 1284(m), 1245(w), 1196(m), 1070(m), 1042(w), 1008(w), 904(s), 877(m), 793(s), 774(m), 691(m), 611(m). UV−vis (toluene), λ_{max} (ε, M^{-1} cm^{-1}): 300 (24600), 440 (13500), 840 (7300).

Ni(bu$_4$phenoxon)$_2$, ***4*** *(M = Ni).* For the preparation of this complex, $Ni(CH_3COO)_2 \cdot 4H_2O$ (6.2 mg, 0.0025 mmol) was used. Green crystals (yield 18.6 mg, 80%). Mp > 360 °C. Anal. Calculated for $C_{56}H_{76}N_2O_6Ni$: C, 72.18; H, 8.22; N, 3.01; Ni, 6.30 Found: C, 72.20; H, 8.21; N, 3.07; Ni, 6.28. ^{1}H NMR (toluene-d$_8$, 30 °C): δ = −0.62 (b, 36H, *tert*-Bu), 2.94 (s, 36H, *tert*-Bu), 24.10 (b, 4H, arom.) ppm. IR(cm^{-1}): 1592(m), 1546(s), 1505(m), 1450(m), 1399(m), 1356(w), 1331(w),

dx.doi.org/10.1021/ic2004062 |*Inorg. Chem.* 2011, 50, 7022–7032

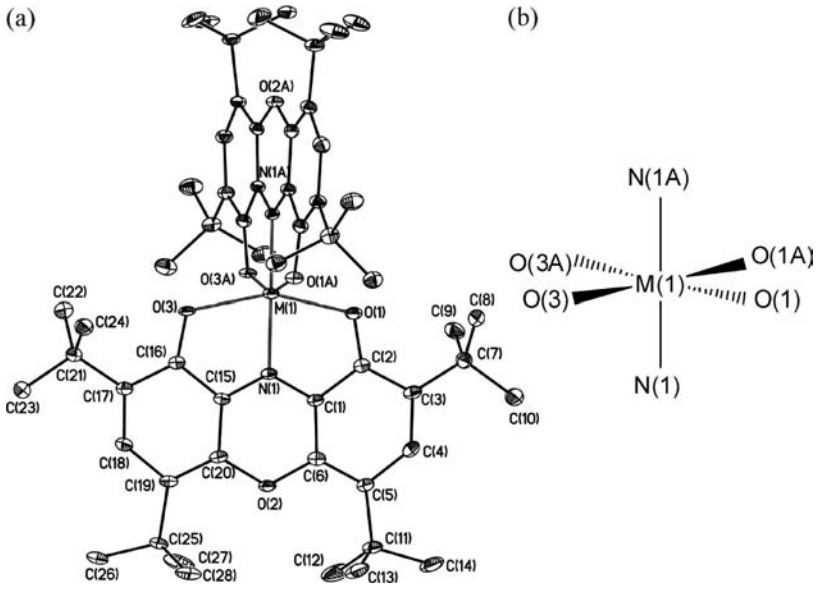

Figure 3. (a) General molecular structure with the numeration of atoms common to all six complexes **4** (M = Mn, Fe, Co, Ni, Cu, Zn). Hydrogen atoms are omitted for clarity. Thermal ellipsoids are shown in 50% probability; (b) Octahedral configuration of the central metal atom (no trigonal distortions are shown). Important bond lengths and valence angles are listed in Table 3.

Table 3. Selected Bond Lengths (Å) and Bond Angles (deg) for Complexes 4

bond, angle	Mn	Fe	Co	Ni	Cu	Zn
M−N(1)	2.164(1)	2.017(3)−2.023(3)	1.989(2)	1.945(3)	1.939(2)	2.020(1)
M−O(1)	2.222(1)	2.109(3)−2.109(3)	2.148(1)	2.134(2)	2.186(2)	2.211(1)
M−O(3)	2.263(1)	2.099(3)	2.154(1)	2.147(2)	2.189(2)	2.192(1)
O(1)−C(2)	1.275(2)	1.285(5)−1.296(5)	1.282(2)	1.294(4)	1.282(3)	1.267(2)
O(3)−C(16)	1.266(2)	1.294(5)	1.274(2)	1.286(4)	1.269(3)	1.272(2)
O(2)−C(20)	1.398(2)	1.399(5)−1.401(5)	1.391(2)	1.395(4)	1.380(2)	1.395(2)
O(2)−C(6)	1.393(2)	1.399(5)−1.408(5)	1.387(3)	1.390(4)	1.382(2)	1.395(2)
N(1)−C(1)	1.327(2)	1.320(5)−1.323(5)	1.315(3)	1.326(4)	1.328(3)	1.316(2)
N(1)−C(15)	1.313(2)	1.318(5)−1.333(5)	1.327(3)	1.320(4)	1.304(3)	1.325(2)
C(1)N(1)C(15)	121.5(2)	120.7(4)−121.2(4)	121.7(2)	122.7(2)	122.7(2)	122.2(1)
O(1)C(2)C(1)	118.4(2)	116.2(4)−116.6(4)	117.7(2)	117.5(3)	118.1(2)	118.1(2)
O(3)C(16)C(15)	118.1(2)	116.1(4)−117.0(4)	117.6(2)	117.7(3)	117.2(2)	118.3(1)
MO(3)C(16)	115.8(1)	115.3(3)	113.0(1)	111.3(2)	110.78(15)	112.5(1)
MO(1)C(2)	116.3(1)	115.9(3)	112.7(1)	111.3(2)	109.99(15)	112.4(1)
N(1)MO(1)	72.40(6)	75.2(1)−75.4(1)	76.80(6)	78.4(1)	78.24(7)	75.75(5)
N(1)MO(3)	71.78(6)	75.3(1)−75.7(1)	76.37(6)	77.8(1)	77.56(7)	76.21(5)
τ	82.9	94.6	88.5	88.8	88.6	88.4

1287(s), 1247(m), 1199(m), 1161(m), 1070(m), 1042(w), 1038(m), 1003(w), 933(s), 905(m), 797(s), 743(s), 696(m). UV−vis (toluene), λ_{max} (ε, M^{-1} cm^{-1}): 297 (28950), 408 (32500), 792 (22000), 883sh.

Cu(bu$_4$phenoxon)$_2$, ***4*** *(M = Cu).* For the preparation of this complex, $Cu(CH_3COO)_2 \cdot H_2O$ (5.0 mg, 0.0025 mmol) was used. Blue crystals (yield 19.4 mg, 83%). Mp 345−346 °C. Anal. Calculated for $C_{56}H_{76}N_2O_6Mn$: C, 71.80; H, 8.18; N, 2.99; Cu, 6.78 Found: C, 71.21; H, 8.10; N, 2.99; Cu, 6.70. ^{1}H NMR (toluene-d$_8$, 30 °C): δ = 0.64 (s, 36H, *tert*-Bu), 2.87 (b, 36H, *tert*-Bu), 11.79 (b, 4H, arom.) ppm. IR(cm^{-1}):1593(m), 1544(s), 1505(m), 14440(m), 1397(m), 1356(w), 1331(w), 1285(s),1247(m),1199(m), 1199(m), 1161(m), 1073(m), 1035(m), 100(w), 932(s), 905(m), 742(m), 697(m), 616(s). UV−vis (toluene), λ_{max} (ε, M^{-1} cm^{-1}): 298 (18700), 410 (17500), 750 (13800), 925sh.

Zn(bu$_4$phenoxon)$_2$, ***4*** *(M = Zn).* For the preparation of this complex, $Zn(CH_3COO)_2 \cdot 2H_2O$ (5.5 mg, 0.0025 mmol) was used. Blue-green crystals (yield 19.2 mg, 82%). Mp > 360 °C. Anal. Calculated for $C_{56}H_{76}N_2O_6Zn$: C, 71.66; H, 8.16; N, 2.98; Zn, 6.97 Found: C, 71.63; H, 8.05; N, 3.07; Zn, 6.90. ^{1}H NMR ($CDCl_3$, 25 °C:δ = 1.24 (s, 36 H, *tert*-Bu); 1.45 (s, 36 H, *tert*-Bu), 7.41 (s, 4H, arom.) ppm. IR(cm^{-1}): 1595(m), 1514(w), 1457(m), 1397(m), 1355(w), 1333(w), 1284(s), 1247(m), 1199(s), 1162(m), 1071(m), 1035(m), 1000(w), 903(s), 877(m), 797(s), 774(s), 742(m), 696(m), 612(s). UV−vis (toluene), λ_{max} (ε, M^{-1} cm^{-1}): 300 (17800), 411 (17850), 739 (14800), 805sh.

Physical Methods. ^{1}H NMR spectra were collected on Bruker Avance 600 MHz spectrometer in dry, degassed $CDCl_3$ or toluene-d$_8$ and referenced to tetramethylsilane (TMS). Temperature stabilization was maintained with the accuracy ±0.1 °C. All chemical shifts are

dx.doi.org/10.1021/ic2004062 |*Inorg. Chem.* 2011, 50, 7022–7032

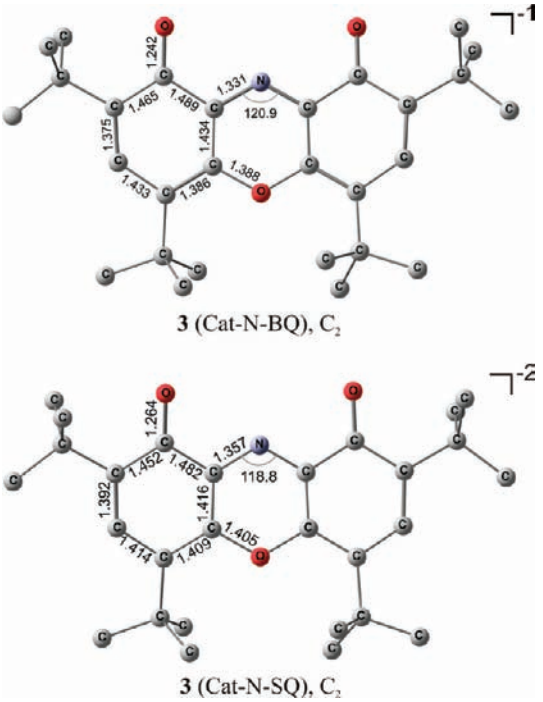

Figure 4. Optimized geometries of tetra-(*tert*-butyl)-9-hydroxyphenoxazin-1-on-9-olate ligand **3** in the anion and radical-dianion oxidation states calculated by the B3LYP*/6-311++G(d,p) method. Here and in the subsequent figures bond lengths are given in Å and angles in degrees and hydrogen atoms are omitted.

Table 4. Total Energies (E_{tot}) and Relative Energies (ΔE) As Calculated by the DFT B3LYP*/6-311++G(d,p) Method for the Isomers of Metal Complexes 4

structure	E_{tot}, a.u.	ΔE, kJ mol^{-1}
4 (M = Mn)-HS, Mn^{II}(Cat-N-BQ)$_2$	−3890.47716	0.0
4 (M = Mn)-LS, Mn^{IV}(Cat-N-SQ)$_2$	−3890.47231	12.7
4 (M = Fe)-HS, Fe^{II}(Cat-N-BQ)$_2$	−4003.16514	0.0
4 (M = Fe)-LS, Fe^{II}(Cat-N-BQ)$_2$	−4003.15753	20.0
4 (M = Co)-HS, Co^{II}(Cat-N-BQ)$_2$	−4122.19593	0.0
4 (M = Co)-LS, Co^{II}(Cat-N-BQ)$_2$	−4122.19083	13.4
4 (M = Ni), Ni^{II}(Cat-N-BQ)$_2$	−4247.72823	
4 (M = Cu), Cu^{II}(Cat-N-BQ)$_2$	−4379.86905	
4 (M = Zn), Zn^{II}(Cat-N-BQ)$_2$	−4518.74351	

reported using the standard δ notation in parts per million. Perpendicular-mode X-band EPR spectra were registered using a Bruker EMX 10/12 spectrometer and analyzed with help of the Bruker WinEPR SimFonia program package. IR spectra were recorded on Varian 3100 FT-IR, Excalibur Series instrument by means of Attenuated Total Reflectance (ATR) method. UV−vis spectra were recorded on an Agilent Technologies HP-8453 spectrophotometer. The magnetization measurements in the solid state were performed in the 77−298 K temperature range with an originally designed Faraday magnetometer. The diamagnetic corrections of the molar magnetic susceptibilities were accounted for using Pascal's constants. Magnetic moments of complexes **4** in solution were determined based on the Evans's method.[12]

Crystallographic Methods. Single crystals of complexes **4** were grown by slow evaporation from benzene solutions. X-ray diffraction data were collected with a Bruker Smart Apex II CCD diffractometer

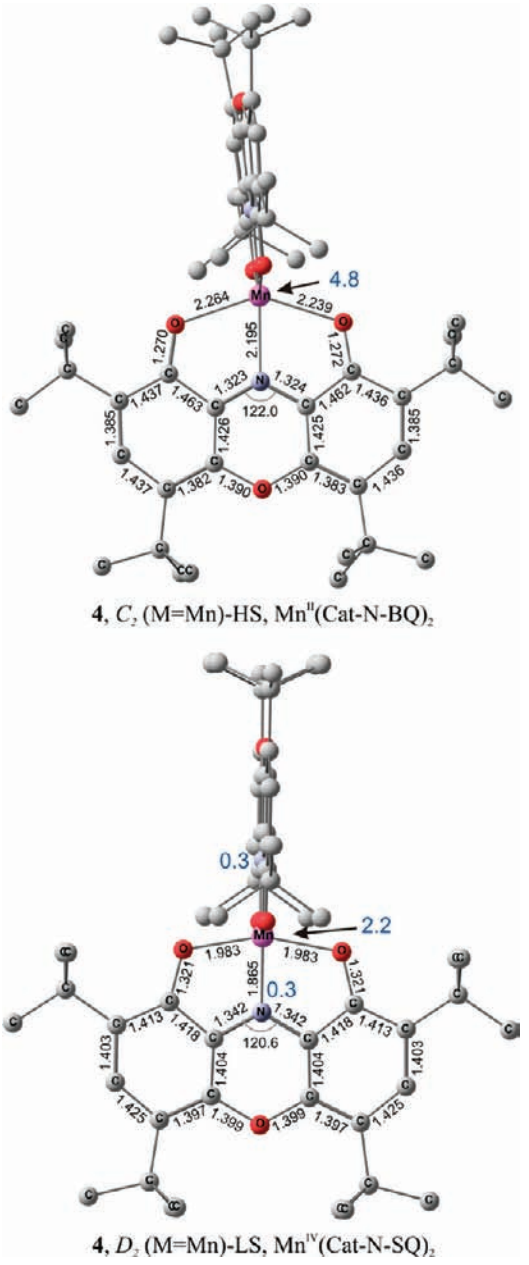

Figure 5. Optimized geometries of redox isomeric forms of complex **4** (M = Mn) as calculated by the DFT B3LYP*/6-311++G(d,p) method. The upper structure corresponds to the experimentally observed isomer. The values of spin densities are shown by blue numerals.

[(λ(MoKα)=0.71072], ω-scans] at 100 K. The substantial redundancy in data allows empirical absorption correction to be performed with SADABS,[13] using multiple measurements of equivalent reflections. The structures were solved by direct methods and refined by the full-matrix least-squares technique against F^2 in the anisotropic-isotropic approximation. The positions of hydrogen atoms were calculated from the geometrical point of view and refined with the riding model. All calculations were performed with the SHELXTL software package.[14] Crystal data and structure refinement parameters are listed in Table 1.

Computational Details. All density functional theory (DFT) calculations were performed by means of the Gaussian 03 program package[15] using the modified B3LYP* functional[16] known to provide for more accurate data on the relative energies of the electronic states with

dx.doi.org/10.1021/ic2004062 |*Inorg. Chem.* 2011, 50, 7022–7032

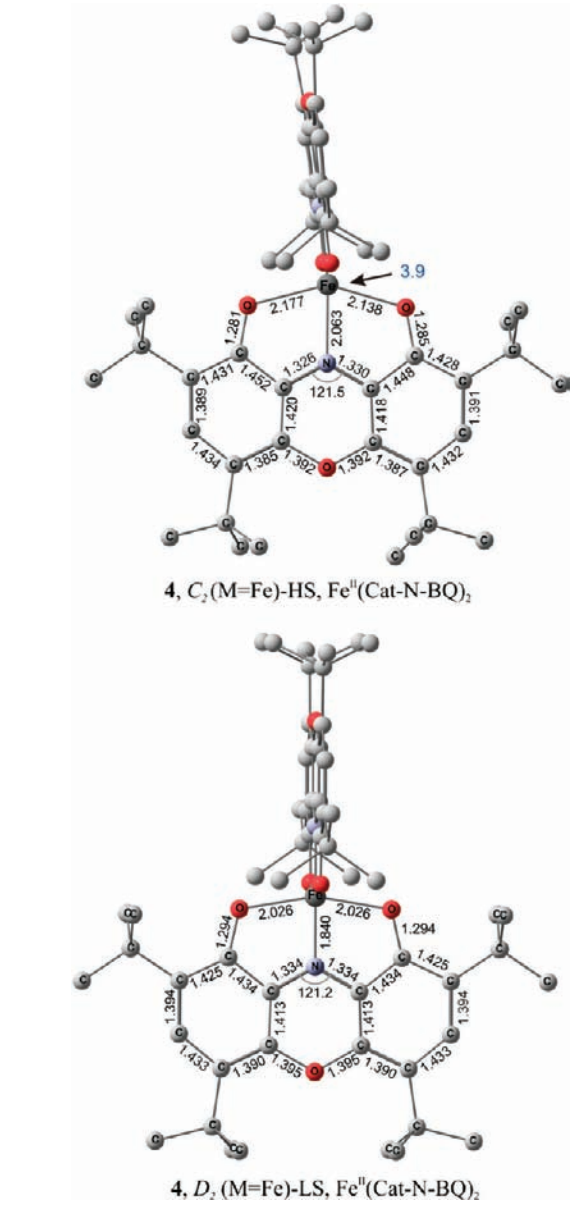

Figure 6. Optimized geometries of the isomeric forms of complex **4** (M = Fe) as calculated by the DFT B3LYP*/6-311++G(d,p) method. The upper structure corresponds to the experimentally observed isomer. The value of spin density at the metal is shown by a blue numeral.

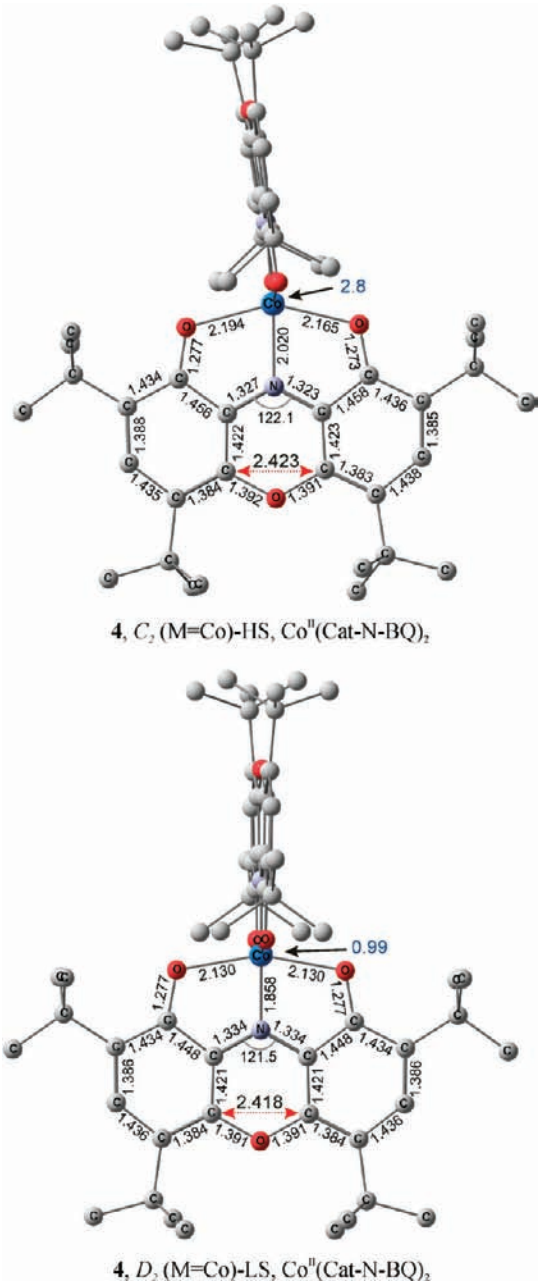

Figure 7. Optimized geometries of the isomeric forms of complex **4** (M = Co) as calculated by the DFT B3LYP*/6-311++G(d,p) method. The upper structure corresponds to the experimentally observed isomer. The dashed line denotes the distance between the C(6)−C(20) atoms of the oxazine ring. The value of spin density at the metal is shown by a blue numeral.

different multiplicities.[17] The standard 6-311++G(d,p) basis set, which reproduces well the energy parameters of a number of previously studied spin-forbidden intramolecular rearrangements,[9,18] was employed for all atoms. The stationary points on the potential PESs were located by full geometry optimization and checked for the stabilities of Hartree−Fock solutions.

RESULTS AND DISCUSSION

Structural Characterization of M(bu$_4$phenoxon)$_2$ Complexes 4 (M = Mn, Fe, Co, Ni, Cu, Zn). The values of effective magnetic moments of complexes **4** (M = Mn, Fe, Co, Ni, Cu) measured in the solid state in the temperature range of 77−298 K and in toluene solution in the temperature range of 183−373 K (Table 2) remain virtually unchanged. This finding bears clear witness to stabilization of the high-spin ground states of the Mn, Fe, Co, and Ni complexes **4** as exemplified below by the case of Co complex, the only observed form of which is represented by the high-spin Co^{II}(Cat-N-BQ)$_2$ isomer. The isotropically shifted ^{1}H NMR spectrum of this complex shown in the region of *tert*-butyl groups (Figure 2) strictly adheres to the Curie−Weiss law.

The high-spin M^{II}(Cat-N-BQ)$_2$ structure of the synthesized complexes **4** (M = Mn, Fe, Co) is consistent with the results of the X-ray diffraction analysis of their molecular and crystal structures summarized in Figure 3 and Table 3. The crystallographic

dx.doi.org/10.1021/ic2004062 |*Inorg. Chem.* 2011, 50, 7022–7032

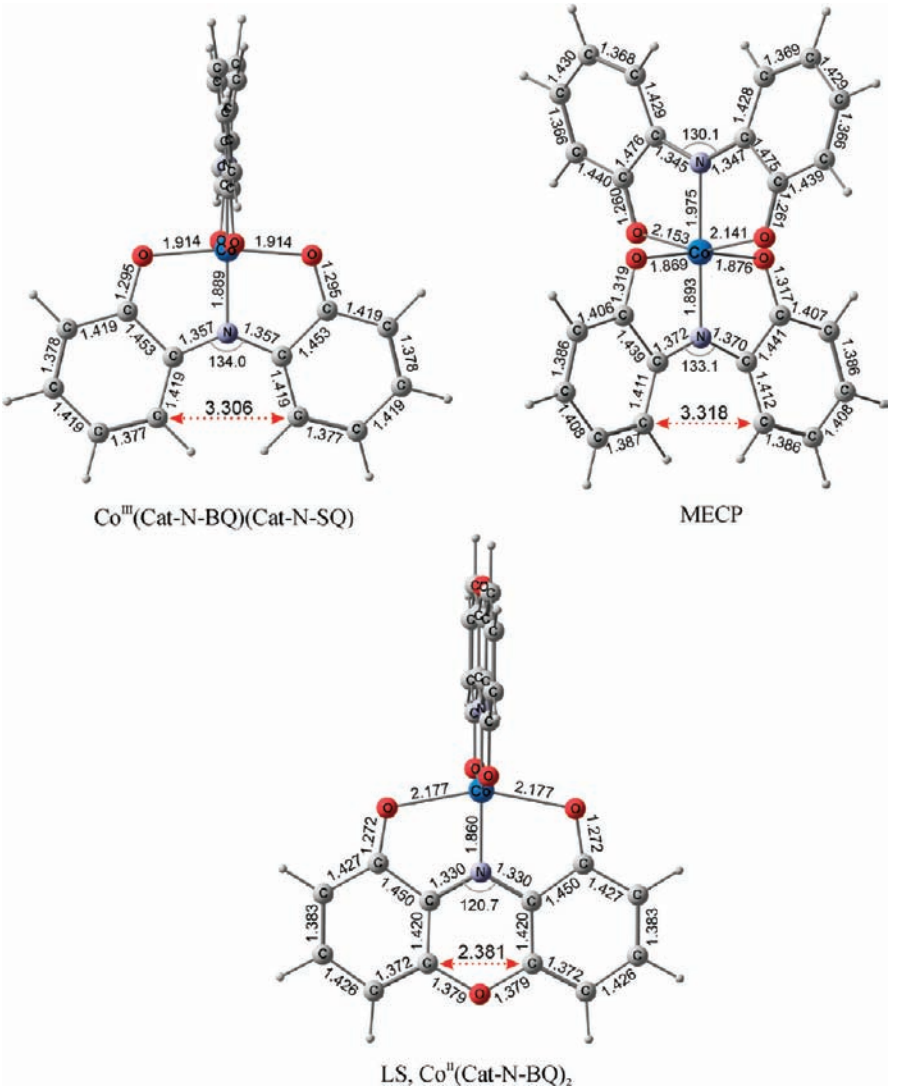

Figure 8. Molecular structures of the Co^{III}(Cat-N-BQ)(Cat-N-SQ) redox isomer of *bis*-(iminoquinonephenolate) Co and MECP for its conversion to the high-spin isomeric form located on the seam of the intersecting doublet and quartet PESs using the B3LYP*/6-311++G(d,p) method.[9] For the comparison, the optimized geometry of the fully analogous (containing no *tert*-butyl groups) *bis*-(oxyphenoxazinonolate) Co has been calculated at the same level of approximation. The dashed lines denote the distances between the carbon atoms corresponding to the C(6) and C(20) positions in the oxazine ring in the general formula in Figure 3a.

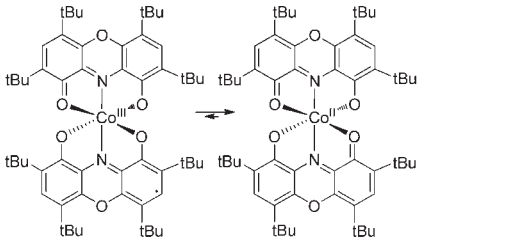

study showed that the two ligands occupy meridional sites of an octahedron. Complexes **4** (M = Co, Ni, Cu and Zn) crystallize as solvates with six benzene molecules. Taking into account that they have the same space group *Pbcn* with the metal atom lying on the 2-fold axis ($Z = 4$, $Z' = 0.5$) and similar cell dimensions (Table 1), these complexes can be considered isostructural. In contrast, the complexes **4** (M = Mn and Fe) crystallize without solvate molecules, but only in the case of **4** (M = Fe) the metal atom occupies the general position, while for the manganese analogue (M = Mn) the symmetry of the complex is also C_2.

In all the complexes, because of the decrease in the bond angles O(1)MN(1) (72.40−78.24(7)°) and O(3)MN(1) (71.78(6)−77.8(1)°) (Table 3) the octahedral configuration is characterized by significant trigonal distortion. The dihedral angle between the two ligands (τ) varies in the narrow range 82.9−94.6° and is likely to be governed by crystal packing. The τ values for the isostructural complexes are, indeed, equal. The ligands, not counting methyl groups, are almost planar. In the complexes, the principal bond lengths within the ligand moieties are rather similar and are almost unaffected by the nature of the metal atom. In particular, C_6-rings are characterized by the pronounced alternation of the bond lengths with shorter C(3)−C(4), C(5)−C(6) and C(17)−C(18), C(19)−C(20) bonds. The same is true for the C−O, C−N bonds and C−N−C

dx.doi.org/10.1021/ic2004062 |*Inorg. Chem.* 2011, 50, 7022–7032

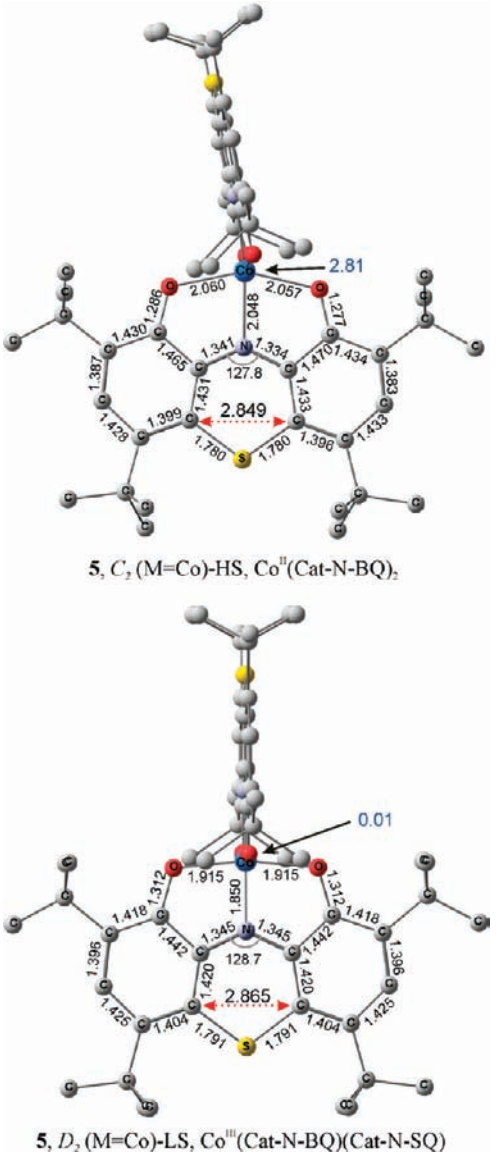

Figure 9. Optimized geometries of *bis*-(oxyphenothiazinonolate) Co complexes **5** (M = Co) as calculated by the DFT B3LYP*/6-31G(d,p) method. The lower structure corresponds to the ground state electromeric form. The dashed line denotes the distance between the C(6)−C(20) atoms of the phenothiazinone ring. The values of spin density at the metal atoms are shown by blue numerals.

bond angles. All these geometric parameters, although varying in the narrow range, cannot be directly interconnected with the M−O and M−N bond lengths.

It should be noted that the above bond lengths in the complexes can be partly affected by the C_2 symmetry of the complexes; hence, we cannot exclude the presence of a symmetry imposed disorder. Indeed, the analysis of the principal anisotropic displacement parameters (see Supporting Information, Figure S1) has revealed that their ratio (2.57−2.74) in complexes **4** (M = Co, Ni, Cu and Zn) is significantly greater than the corresponding value (1.78) for **4** (M = Fe) in which metal atom occupies the general position. Unfortunately, the possible variation of the M−O bond because of such a disorder is rather small and cannot be unambiguously judged by the Hirshfeld rigid bond test.[20] Thus, to additionally verify that the observed geometric parameters are not affected by the symmetry imposed by disorder (see. for example, ref 21), we have performed the DFT calculations of the above complexes.

The Zn−O and Zn−N bond lengths in **4** (M = Zn) are slightly longer than those (2.119(2)−1.255(2) and 2.074(2)−2.086(2)Å, respectively) in the diamagnetic green form of bis(iminoquinonephenolate) Zn(II).[22a] Elongation of the metal−ligand coordination bonds in complexes **4** compared to the corresponding bis(iminoquinonephenolate) analogues is also characteristic of the Co, Ni, and Fe complexes.[22b,c] This trend is a consequence of the high-spin ground electronic state of **4** caused by the rigidity of the tricyclic structure of the phenoxazinone ligand **3**.

DFT Calculations of the High-Spin and Low-Spin Isomeric Structures of Complexes 4 (M = Mn, Fe, Co, Ni, Cu, Zn). As seen from the calculated structures of the radical-anion and dianion of **3**, which represent the most likely forms of this ligand in the redox-active complexes, their geometries are strongly dependent on the oxidation state (Figure 4). The differences in the lengths of the CC bonds (noninclusive into the coordination sites of metal complexes **4**) in **3** (Cat-N-BQ) achieve 0.015−0.020 Å, whereas the alternation of these in **3** (Cat-N-SQ) is appreciably lower. In accordance with the X-ray structural data on the ligand **3**[11a] their tricyclic frameworks are substantially distorted because of the perceptible repulsive interactions between the bulky *tert*-butyl groups in the positions 4 and 6. These steric interactions exert also significant effects on the geometries of the metal complexes **4**. Thus, the calculations performed on the model structures of complexes **4** stripped of all *tert*-butyl groups resulted in the substantial disparities with the experimental molecular geometries (Table 3). It was, therefore, necessary to conduct the calculations of the energy and structural parameters of complexes **4** without any simplifications of their molecular forms. The results obtained are collected in Table 4 and presented in Figures 5−7, 9.

*Mn(bu$_4$phenoxon)$_2$, **4** (M = Mn).* The ground state structure **4** (M = Mn)-HS of the manganese complex corresponds to a minimum located on the sextet PES. The calculated geometry shown in Figure 5 is in reasonable agreement with the X-ray crystallographic data (Table 3). The experimentally determined magnetic moment (μ_{eff} = 5.88 μ_B) is compatible with two possible electromeric[5] forms of the same multiplicity: the high-spin Mn(II) complex or the Mn(III) complex with feromagnetically coupled unpaired electrons of the metal and the ligand in the radical-dianion oxidation state. The calculated distribution of spin density, which is almost fully concentrated on the metal center (q_s = 4.8), as well as the observed independence of μ_{eff} from temperature bear clear evidence to the former's electromeric structure. This assignment is proven also by the close values of the intraligand CC bonds in **4** (M = Mn)-HS and the anionic form of the ligand **3** (Cat-N-BQ). The search for the redox isomeric form of **4** has led to the low-spin D_{2d} symmetry structure **4** (M = Mn)-LS located on the doublet PES. The calculated lengths of the coordination Mn−O and Mn−N bonds, 1.983 and 1.865 Å, respectively, are equally characteristic of low spin Mn(II), Mn(III), and Mn(IV) complexes and, thus, are not indicative of the oxidation state of the central atom. On the other hand, the calculated distribution of spin density can best of all be described by the structural formula with three unpaired electrons at the metal center and one unpaired electron at each of the ligands (Figure 5). Such the structure may be assigned to either a Mn(II) complex with an intermediate spin or a high-spin Mn(IV) complex. However, the spin density localized

dx.doi.org/10.1021/ic2004062 |*Inorg. Chem.* 2011, 50, 7022–7032

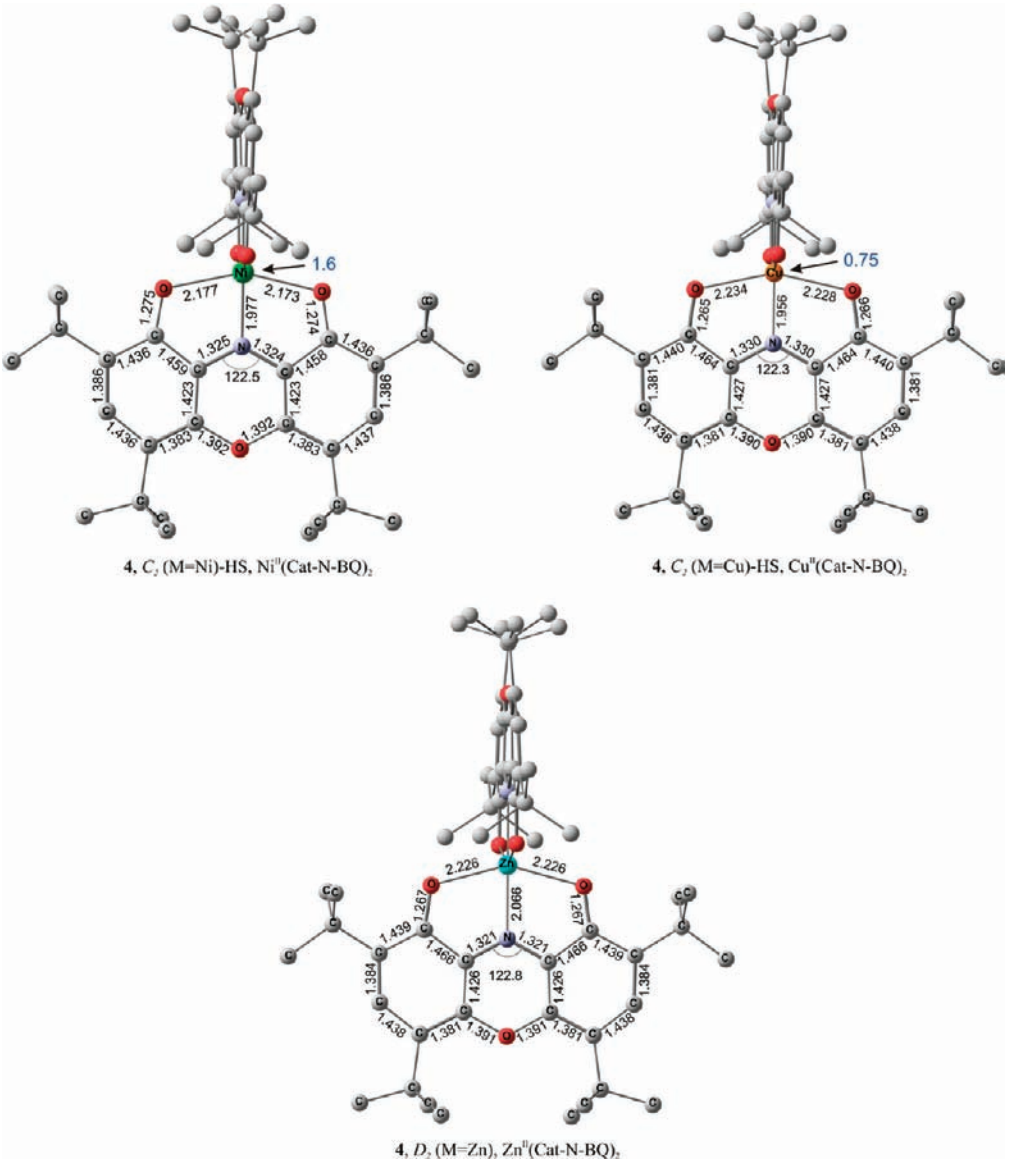

Figure 10. Optimized geometries of the ground state structures of complexes **4** (M = Ni, Cu, Zn) as calculated by the DFT B3LYP*/6-311++G(d,p) method. The values of spin density at the metal atoms are shown by blue numerals.

at the ligands points to their radical-dianion form **3** (Cat-N-SQ) (Figure 4) and, therefore, to the low-spin Mn^{IV}[(SQ-N-Cat]$_2$ structure of **4** (M = Mn)-LS characterized by strong antiferromagnetic coupling of the unpaired electrons. Since the low-spin structure **4** (M = Mn)-LS is 12.7 kJ mol^{-1} destabilized with respect to the high-spin structure **4** (M = Mn)-HS (Table 4) no thermally induced valence tautomeric interconversion of these redox isomer may be expected.

*Fe(bu$_4$phenoxon)$_2$, **4** (M = Fe).* As for the manganese complex, the low-spin isomer of the iron complex **4** (M = Fe)-LS located on the singlet PES is energy disfavored with respect to its high-spin counterpart **4** (M = Fe)-HS located on the quintet PES (Table 4, Figure 6). Whereas the intraligand geometries of **4** (M = Fe)-HS and **4** (M = Fe)-LS are very similar, the lengths of the coordination bonds in these structures notably differ. The stability of the Hartree−Fock solution for the closed shell structure **4** (M = Fe)-LS confirms the low-spin Fe(II) form of this complex. No low-spin isomeric form of **4** (M = Fe) with a Fe(III) center has been revealed by the calculations. Therefore, no valence tautomerism of **4** (M = Fe) is predicted by the calculations.

*Co(bu$_4$phenoxon)$_2$, **4** (M = Co).* The ground state form of the complex **4** (M = Co) is represented by the high-spin structure **4** (M = Co)-HS located on the quartet PES (Figure 7). The calculated geometric parameters of **4** (M = Co)-HS reproduce well those experimentally determined parameters (Table 3), including the subtle differences in the metal−ligand Co−O bonds in the *pseudo*-octahedral coordination site. In full agreement with the measurements of μ_{eff} (three unpaired electrons), spin density is almost fully localized on the metal (q_s = 2.8). A low-spin structure **4** (M = Co)-LS with a single electron localized on the metal has been located on the doublet PES. It is 13.4 kJ mol^{-1} energy richer than the ground state high-spin structure **4** (M = Co)-HS. This makes it highly improbable to observe valence tautomeric or spin-crossover rearrangements in the case of the Co complex **4**. Worth noting is the significant elongation of

dx.doi.org/10.1021/ic2004062 |*Inorg. Chem.* 2011, 50, 7022–7032

the Co−O bonds (2.13 Å) in **4** (M = Co)-HS as compared with the typical values (1.8−1.9 Å) found for these bonds in the low-spin Co(III) and Co(II) complexes.[23]

The Co−O bonds in the ground state high-spin structure of **4** (M = Co) are significantly (∼ 0.2 Å) stretched compared to those in the low-spin redox isomer of its nearest structural analogue, *bis*-(iminoquinonephenolate) Co^{III}(Cat-N-BQ)(Cat-N-SQ), the structure of which is shown in Figure 8. The elongation of metal-to-ligand coordination bonds in the high-spin forms is a characteristic property of all transition metal complexes.[24] In **4** (M = Co), it is caused by the rigidity of the heterocyclic framework of hydroxyphenoxazinone ligand **3** that precludes shortening the metal−ligand bonds to the values optimal for the low-spin structures. An important consequence of the structural rigidity of the stems from the results of our previous DFT B3LYP*/6-311++G(d,p) study of the valence tautomeric rearrangements of *bis*-(iminoquinonephenolate) Co.[9] In agreement with the experimental data,[8e] the calculations correctly predict the energy preference (by 17.6 kJ mol^{-1}) of the low-spin Co^{III}(Cat-N-BQ)(Cat-N-SQ) structure. As shown in Figure 8, the distinctive structural features of the low-spin isomer of *bis*-(iminoquinonephenolate) Co and the MECP[6] determining the energy barrier (51.8 kJ mol^{-1}) against its thermally initiated rearrangement to the high-spin redox isomer Co^{II}(Cat-N-BQ)$_2$ are the high values (130.1°−134.0°) of the valence CNC angles and the significant displacement separation of the two arene rings (3.1−3.3 Å) inaccessible in complexes **4** (M = Co) based on the rigid tricyclic ligands. These values are sharply contrasted with the calculated (124.1°−122.8°) and experimentally determined C(1)−N(1)−C(15) angles and C(6)−C(20) distances (Figure 7, Table 3) of Co and other complexes **4**. The rigidity of the ligand framework of complexes **4** sterically hinders the widening of their central rings necessary for the contraction of the M−O bonds in the low-spin ground state structure and imposes a strict limit on the increase in the CNC angles as required for the formation of a suitable MECP structure.

Structural modification of the ligand structure expected to provide for stabilization of the low-spin electronic states of derivatives of complexes **4** must be primarily associated with the search for compounds with the increased intracyclic CNC angle. One way to this goal, which is currently under study in our laboratory, consists in the replacement of an oxygen atom in the central 1,4-oxazine ring of **3** by a bulkier sulfur atom. As proven by our preliminary DFT calculations performed at this stage with a modest 6-31G(d,p) basis set, the C(6)−C(20) distance in the low-spin structure **5** (M = Co)-LS located on the doublet PES is appreciably longer and the Co−O coordination bonds shorter than those in **4** Co^{II}(Cat-N-BQ)$_2$ (Figure 7). As a result, the low-spin isomer is predicted to be preferred by 19 kJ mol^{-1} energy to its high-spin form **5** (M = Co)-HS located on the quartet PES. Such an energy gap makes possible valence tautomeric rearrangements between the redox isomers of **5** (M = Co) caused by the intramolecular ligand-to-metal electron transfer. Whereas in **5** (M = Co)-LS an unpaired electron is delocalized over the ligands, which allows one to assign its structure to the CoIII(Cat-N-BQ)(Cat-N-SQ) type, in the high-spin isomer all three unpaired electrons are localized on the metal center which is in accord with the high-spin Co(II) electronic state. The calculated structures of the redox isomers of **5** (M = Co) are shown in Figure 9.

It may, thus, be concluded that it is the rigidity of the molecular framework of hydroxyphenoxazinone ligands **3** that represents the principal factor determining relative stabilization of the high-spin ground state of complexes **4** and retarding possible rearrangements between their redox isomeric forms as well.

*Ni(bu$_4$phenoxon)$_2$, **4** (M = Ni), Cu(bu$_4$phenoxon)$_2$, **4** (M = Cu), and Zn(bu$_4$phenoxon)$_2$ **4** (M = Zn).* The ground state structures of the nickel **4** (M = Ni), copper **4** (M = Cu), and zinc **4** (M = Zn) complexes are shown on Figure 10. The calculated geometries are in reasonable agreement with the X-ray crystallographic data (Table 3). In contrast with the Co analogue (Figure 7), the M−O bonds in all these complexes are equivalent. The complexes **4** (M = Ni) and **4** (M = Cu) have triplet and doublet ground electronic states, respectively, with spin density mostly localized on the metal centers. Thus, for **4** (M = Cu) 75% of the calculated spin density is concentrated on the copper atom, which is in accord with the value (80%) estimated on the basis of a previous EPR study[11a] of this compound. The calculations have not revealed any stable structure of **4** (M = Cu) with the Cu(I) oxidation state.

CONCLUSION

Because of the steric rigidity of the tricyclic molecular framework 9-hydroxyphenoxazin-1-one ligands **3** represent a specific molecular platform particularly fitted to stabilization of the high-spin ground states of the octahedral tris-chelate d^5-d^9 metal complexes formed on their basis. Because of relative instability of the low-spin electronic states of complexes **4** and because of the strict restrictions (sterically fixed narrow CNC angles and short C(6)−C(20) distances) imposed on the structural evolution of molecules **4** that would lead to the formation of suitable MECP structures, no valence tautomeric rearrangements were observed or predicted to occur for these complexes. The appropriate modifications of the ligand structure that might stabilize the low-spin electronic states of derivatives of complexes **4** and provide for the occurrence of their valence tautomeric rearrangements must be related to the search for compounds with the increased intracyclic CNC angle, for example, such as the derivatives of 9-hydroxyphenothiazin-1-one.

ASSOCIATED CONTENT

Supporting Information. X-ray crystallographic data files in CIF format for **4**. Details of the theoretical calculations for **3**-**4**, including absolute energies, and optimized geometries. This material is available free of charge via the Internet at http://pubs.acs.org.

AUTHOR INFORMATION

Corresponding Author

*E-mail: minkin@ipoc.rsu.ru. Phone: +7(863)2434700.

ACKNOWLEDGMENT

This work has been supported by the Ministry of Education and Science RF (Contract P2260 and grant N. Sh. 3233. 2010.3).

REFERENCES

(1) (a) Pierpont, C. G. *Coord. Chem. Rev.* **2001**, *216*−*217*, 99–125. (b) Gütlich, P.; Garcia, Y.; Woike, T. *Coord. Chem. Rev.* **2001**, *219*−*221*, 839–879. (c) Hendrickson, D. N.; C.G. Pierpont, C. G. *Top. Curr. Chem.* **2004**, *234*, 63–95. (d) Evangelio, E.; Ruiz-Molina, D. *C. R. Chim.* **2008**, 1137–1154.

(2) (a) Dei, A.; Gatteschi, D.; Sangregorio, C.; Sorace, L. *Acc. Chem. Res.* **2004**, *37*, 827–835. (b) Sato, O.; Tao, J.; Zhang, Y. Z. *Angew. Chem., Int. Ed.* **2007**, *46*, 2152–2187.

(3) (a) Chirik, P. J.; Wieghardt, K. *Science* **2010**, *327*, 794–795. (b) Boyer, J. L.; Rochford, J.; Tsai, M.-K.; Muckerman, J. T.; Fujita, E. *Coord. Chem. Rev.* **2010**, *254*, 309–330.

(4) (a) Jørgensen, C. K. *Coord. Chem. Rev.* **1966**, *1*, 164–178. (b) Butin, K. P.; Beloglazkina, E. K.; Zyk, N. V. *Russ. Chem. Rev.* **2005**, *74*, 531–553.

(5) Bally, T. *Nat. Chem.* **2010**, *2*, 165–166.

(6) Harvey, J. N.; Aschi, M.; Schwarz, H.; Koch, W. *Theor. Chem. Acc.* **1998**, *99*, 95–99.

(7) Buchanan, R. M.; Pierpont, C. G. *J. Am. Chem. Soc.* **1980**, *102*, 4951–4957.

(8) (a) Girgis, A. Y.; Balch, A. L. *Inorg. Chem.* **1975**, *14*, 2724–2727. (b) Larsen, S. K.; Pierpont, C. G. *J. Am. Chem. Soc.* **1988**, *110*, 1827–1832. (c) Bruni, S.; Caneschi, A.; Cariati, F.; Delfs, C.; Dei, A.; Gatteschi, D. *J. Am. Chem. Soc.* **1994**, *116*, 1388–1394. (d) Speier, G.; Csihony, J.; Whalen, A. M.; Pierpont, C. G. *Inorg. Chem.* **1996**, *35*, 3519–3524. (e) Caneschi, A.; Cornia, A.; Dei, A. *Inorg. Chem.* **1998**, *37*, 3419–3421. (f) Chaudhuri, P.; Hess, M.; Weihenmüller, T.; Wieghardt, K. *Angew. Chem., Int. Ed.* **1999**, *38*, 1095–1098.

(9) Koval, V. V.; Starikov, A. G.; Minkin, V. I.; Minyaev, R. M. *Doklady Chem.* **2010**, *435*, 319–323.

(10) Evangelio, E.; Bonnet, M. L.; Cabañas, M.; Nakano, M.; Sutter, J. P.; Dei, A.; Robert, V.; Ruiz-Molina, D. *Chem.—Eur. J.* **2010**, *16*, 6666–6677.

(11) (a) Simakov, V. I.; Gorbanev, Yu.Yu.; Ivakhnenko, T. E.; Zaletov, V. G.; Lyssenko, K. A.; Starikova, Z. A.; Ivakhnenko, E. P.; Minkin, V. I. *Russ. Chem. Bull.* **2009**, *58*, 1361–1370. (b) Karsanov, I. V.; Ivakhnenko, E. P.; Khandkarova, V. S.; Prokof'ev, A. I.; Rubezhov, A. Z.; Kabachnik, M. I. *J. Organomet. Chem.* **1989**, *379*, 1–25.

(12) Evans, D. F. *J. Chem. Soc.* **1959**, 2003–2005.

(13) (a) Sheldrick, G. M. *SADABS*; Bruker AXS Inc.: Madison, WI, 1997. (b) Sheldrick, G. M. *SHELXTL-97*, Version 5.10; Bruker AXS Inc.: Madison, WI, 1998.

(14) Sheldrick, G. M. *Acta Crystallogr.* **2008**, *A64*, 112–122.

(15) Frisch, M. J.; Trucks, G. W.; Schlegel, H. B.; Scuseria, G. E.; Robb, M. A.; Cheeseman, J. R.; Montgomery, J. A., Jr.; Vreven, T.; Kudin, K. N.; Burant, J. C.; Millam, J. M.; Iyengar, S. S.; Tomasi, J.; Barone, V.; Mennucci, B.; Cossi, M.; Scalmani, G.; Rega, N.; Petersson, G. A.; Nakatsuji, H.; Hada, M.; Ehara, M.; Toyota, K.; Fukuda, R.; Hasegawa, J.; Ishida, M.; Nakajima, T.; Honda, Y.; Kitao, O.; Nakai, H.; Klene, M.; Li, X.; Knox, J. E.; Hratchian, H. P.; Cross, J. B.; Bakken, V.; Adamo, C.; Jaramillo, J.; Gomperts, R.; Stratmann, R. E.; Yazyev, O.; Austin, A. J.; Cammi, R.; Pomelli, C.; Ochterski, J. W.; Ayala, P. Y.; Morokuma, K.; Voth, G. A.; Salvador, P.; Dannenberg, J. J.; Zakrzewski, V. G.; Dapprich, S.; Daniels, A. D.; Strain, M. C.; Farkas, O.; Malick, D. K.; Rabuck, A. D.; Raghavachari, K.; Foresman, J. B.; Ortiz, J. V.; Cui, Q.; Baboul, A. G.; Clifford, S.; Cioslowski, J.; Stefanov, B. B.; Liu, G.; Liashenko, A.; Piskorz, P.; Komaromi, I.; Martin, R. L.; Fox, D. J.; Keith, T.; Al-Laham, M. A.; Peng, C. Y.; Nanayakkara, A.; Challacombe, M.; Gill, P. M. W.; Johnson, B.; Chen, W.; Wong, M. W.; Gonzalez, C.; Pople, J. A. *Gaussian 03*, revision E.01; Gaussian, Inc.: Wallingford, CT, 2004.

(16) Becke, A. D. *J. Chem. Phys.* **1993**, *98*, 5648–5652.

(17) (a) Reiher, M. *Inorg. Chem.* **2002**, *41*, 6928–6935. (b) Reiher, M.; Salomon, O.; Hess, B. A. *Theor. Chem. Acc.* **2001**, *107*, 48–55.

(18) (a) Shiota, Y.; Sato, D.; Juhász, G.; Yoshizawa, K. *J. Phys. Chem. A* **2010**, *114*, 5862–5869. (b) Starikov, A. G.; Minyaev, R. M.; Minkin, V. I. *J. Mol. Struct.: THEOCHEM.* **2009**, *895*, 138–141. (c) Starikov, A. G.; Minkin, V. I.; Minyaev, R. M.; Koval, V. V. *J. Phys. Chem. A.* **2010**, *114*, 7780–7785.

(19) (a) Poddel'sky, A. I.; Cherkasov, V. K.; Abakumov, G. A. *Coord. Chem. Rev.* **2009**, *253*, 291–324. (b) Cui, A.; Takahashi, K.; Fujishima, A.; Sato, O. *J. Photochem. Photobiol. A* **2004**, *161*, 243–246.

(20) Hirshfeld, F. L. *Acta Crystallogr.* **1976**, *32*, 239–244.

(21) (a) Voloshin, Y. Z.; Varzatskii, O. A.; Novikov, V. V.; Strizhakova, N. G.; Vorontsov, I. I.; Vologzhanina, A. V.; Lyssenko, K. A.; Romanenko, G. V.; Fedin, M. V.; Ovcharenko, V. I.; Bubnov, Y. N. *Eur. J. Inorg. Chem.* **2010**, *34*, 5401–5415. (b) Boese, R.; Antipin, M.Yu.; Lyssenko, K. A. *J. Phys. Chem. B* **1998**, *102*, 8654–8660.

(22) (a) Chaudhuri, P.; Hess, M.; Hildenbrandt, K.; Bill, E.; Weyhermüller, T.; Wieghardt, K. *Inorg. Chem.* **1999**, *38*, 2781–2790. (b) Speier, G.; Csihony, J.; Whalen, A. M.; Pierpont, C. G. *Inorg. Chem.* **1996**, *35*, 3519–3524. (c) Simpson, C. L.; Boone, S. R.; Pierpont, C. G. *Inorg. Chem.* **1989**, *28*, 4379–4385.

(23) (a) Larsen, S. K.; Pierpont, C. G. *J. Am. Chem. Soc.* **1988**, *110*, 1827–1832. (b) Ruiz-Molina, D.; Veciana, J.; Wurst, K.; Hendrickson, D. N.; Rovira, C. *Inorg. Chem.* **2000**, *39*, 617–619.

(24) Gavrilova, A. L.; Bosnich, B. *Chem. Rev.* **2004**, *104*, 349–383.